

Local mass transfer and flow visualization around a cylinder in a liquid-solid fluidized bed

Nevenka M. Bošković-Vragolović¹, Danica V. Brzić¹, Katarina S. Šučurović², Rada V. Pjanović¹, Darko R. Jaćimovski² and Radmila V. Garić-Grulović²

¹University of Belgrade, Faculty of Technology and Metallurgy, Belgrade, Serbia

²University of Belgrade, Institute of Chemistry, Technology and Metallurgy - National Institute of the Republic of Serbia, Belgrade, Serbia

Abstract

Adsorption method has been used for flow visualisation and determination of the local and average mass transfer coefficients around a horizontal cylinder in a liquid-solid fluidized bed. The obtained concentration fields on the adsorbent (silica-foils) represent a clear qualitative flow pattern around the cylinder. By comparison of the concentration fields around the cylinder in the single-phase flow and in the fluidized bed, a significant disturbance of the boundary layer by fluidized particles can be observed. Local mass transfer coefficients were shown to be dependent on the angular position around the cylinder with the maximum determined at the angle 140° (measured from the stagnant point 0°). Selected correlations were applied to predict the average mass transfer coefficients and the two best have shown deviations from the experimental data up to 5 %.

Keywords: Mass transfer coefficients; adsorption method; flow past cylinder; concentration fields.

Available on-line at the Journal web address: <http://www.ache.org.rs/HI/>

ORIGINAL SCIENTIFIC PAPER

UDC: 544.552.11:676.026.1

Hem. Ind. 78(3) 147-159 (2024)

1. INTRODUCTION

Liquid-solid fluidized beds (FB) have extensive applications in chemical, biochemical, food and environmental industries. Most of the processes, which are performed in liquid-solid FBs involve mass transfer, like: adsorption/desorption, ion-exchange, chromatographic separations and heterogeneously catalyzed reactions. Fields of application of liquid-solid FBs expand continuously, especially in biotechnological processes where they are used as bioreactors [1] as well as in processes for water and waste-water treatment [2]. In design and operation of liquid-solid FBs, accurate determination of mass transfer rates plays a key role.

Investigations of mass transfer in FB refer commonly to the measurements of mass transfer coefficients (MTC) leading to numerous empirical correlations. One very good review of those correlations has been given by Kalaga *et al.* [3]. Most of the investigators have measured particle-to-liquid MTCs, presenting average MTCs over the surface of the particles [4,5,6]. Some of the correlations have been determined based on the mass transfer between an immersed object and liquid [7,8,9,10] or the column wall and liquid [11,12,13]. In these studies, both local and average values of MTC can be considered. Determination of local MTCs around an immersed object has both phenomenological and practical significance. The values of the local MTCs around the immersed object can help understanding the complex two-phase flow pattern in the vicinity of the object surface. On the other hand, local MTCs are important for processes in liquid-solid FBs with internals, like membrane FBs [14] or electrochemical FB reactors [15].

Local MTCs around an immersed cylinder have been reported in literature for gas-solid fluidized beds [16,17]. However, studies of local MTCs around a cylinder in liquid-solid FBs are lacking.

Adsorption method [18] has already been shown as a very convenient technique for flow visualization [19] and mass transfer studies [20]. The method is based on measurements of the concentration of an adsorbate (an organic dye) on

Corresponding authors: Katarina S. Šučurović, University of Belgrade, Institute of Chemistry, Technology and Metallurgy, National Institute of the Republic of Serbia, Njegoševa 12, 11000 Belgrade, Serbia

Paper received: 23 October 2023; Paper accepted: 9 September 2024; Paper published: 24 September 2024.

E-mail: katarina.sucurovic@ihtm.bg.ac.rs

<https://doi.org/10.2298/HEMIND231023018B>



the adsorbent surface after being shortly exposed to adsorption from a very dilute solution in the regime of mass transfer control. Previous studies on mass transfer around a cylinder in the single phase (liquid) flow by the adsorption method [21], have shown that the concentration boundary layer can be clearly visualized as well as separation of the boundary layer and formation of the wake.

In this work, mass transfer to the horizontal cylinder in a liquid-solid fluidized bed has been studied experimentally by the adsorption method. Visualisation of flow pattern has been used to evaluate the existence of the boundary layer around the cylinder and the extent of its erosion by fluidized particles, by comparison with the flow pattern for the single-phase flow. Local MTCs around the cylinder have been determined for different particle diameters and liquid velocities. Average MTCs have also been determined and compared with the values predicted by selected literature correlations.

2. EXPERIMENTAL

The experimental system is shown in Figure 1. The experiments were conducted in a column of a rectangular cross-section of 140×10 mm and height of 200 mm. A short cylinder with a diameter of 30 mm and a length of 10 mm, was placed horizontally in the column so that it touched the walls. Silica-gel foils (HPTLC LiChrospher Silica gel, Merck, Germany) with a thickness of 0.3 mm, were wrapped around the cylinder body and placed on the flat walls of the column. Particles used for fluidization were glass beads whose properties are given in Table 1. The initial height of the bed was 80 % of the column height. A diluted water solution of methylene blue ($c_0 = 2.5 \text{ mg dm}^{-3}$, $D_{AB}(20^\circ\text{C}) = 5.84 \cdot 10^{-10} \text{ m}^2 \text{ s}^{-1}$) was recirculated through the column by a pump. The flowrate was regulated by a valve and measured by a flowmeter. Duration of the experiments was determined experimentally in order to fulfill the condition of the pure diffusional regime [18], and it was 7 min in the single-phase flow and 5 min in the fluidized bed. After each experiment, the silica gel foils were dried for 24h in dark and subsequently scanned. The scanned images were processed by using the "Sigma Scan Pro 5" software (SigmaScan Software, Jandel Scientific, USA), providing color intensities on the foils.

Table 1. Characteristics of the particles

d_p / mm	$\rho_p / \text{kg m}^{-3}$	$U_{mf} / \text{m s}^{-1}$	$U_t / \text{m s}^{-1}$	ϵ_{mf}
1.2	2922	0.017	0.172	0.42
2.1	2484	0.027	0.313	0.45

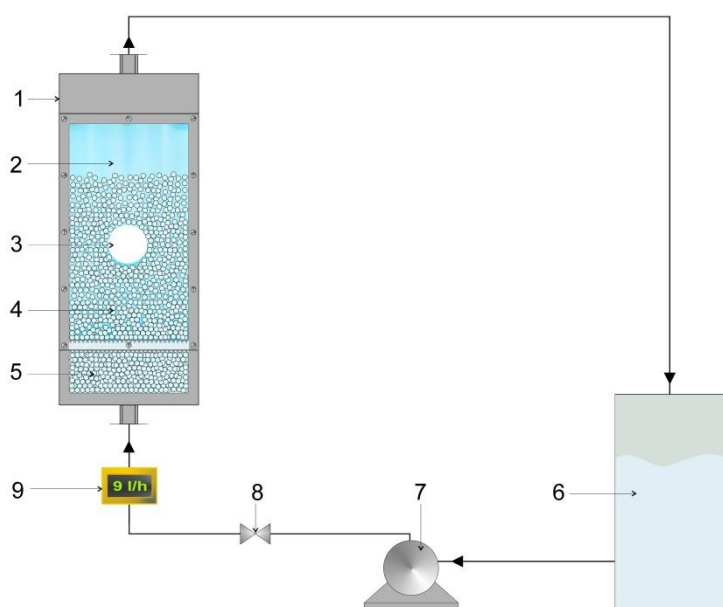


Figure 1. Schematic representation of the experimental set-up: 1 - column, 2 - silica-gel foils, 3 - cylinder, 4 - fluidized bed, 5 - distributor, 6 - tank, 7 - pump, 8 - valve, 9 - flow meter

As it has already been shown in theory of the adsorption method [18], the mass transfer coefficient can be calculated by Equation (1):

$$k = \frac{c_p}{c_0 t} \quad (1)$$

where c_0 is the bulk concentration of the adsorbate, t is the exposure time and c_p is the surface concentration.

The bulk concentration in the aqueous solution of methylene blue c_0 was determined by measuring the intensity of transmitted light at a wavelength of 665 nm by a spectrophotometer (MAPADA UV-3100, China) using a previously determined standard line. The surface concentration c_p was calculated based on the color intensity of the foils by using the previously determined standard line, which represents the function of the surface color intensity on the known surface concentration. The local mass transfer coefficients were determined by using Equation (1) based on the color intensity point by point, while the average mass transfer coefficients were calculated based on the color intensity of the whole surface of the foil.

By previous examination of the expansion of the fluidized bed, dependencies for determining the porosity were defined Equations (2) and (3):

$$\frac{U}{U_t} = 0.61\varepsilon^{1.92} \quad (\text{for } d_p = 1.2 \text{ mm}) \quad (2)$$

$$\frac{U}{U_t} = 0.50\varepsilon^{2.04} \quad (\text{for } d_p = 2.1 \text{ mm}) \quad (3)$$

Ranges of operating conditions in the experiments are shown in Table 2. Total of 17 experiments were performed, while each experiment was performed at least twice for assuring reliability of the measurements.

Table 2. Ranges of operating conditions in the experiments

	$\dot{v} / \text{dm}^3 \text{ min}^{-1}$	Re_c	Re_p	ε
Single phase flow	0.73-7.7	270-290 0	/	/
Fluidized bed	1.8-9.42	680-3600	20-240	0.44-0.85

3. RESULTS AND DISCUSSION

3. 1. Flow visualization

Application of the adsorption method provided determination of the concentration fields on silica-foils, where the colour intensity is directly proportional to the adsorbate concentration. Figures 2, 3 and 4 show chromatograms that correspond to the concentration fields in two views - the first is a scanned foil, and the second is a foil with marked fields of the same colour intensity. Figure 2 represents comparison of the concentration fields on the column wall for the single-phase flow around the cylinder and in the fluidized bed at almost the same liquid velocity.

In the single-phase flow, the concentration field provides a clear visualization of the flow pattern, which represents a typical discontinuous boundary layer around an immersed object indicated by a lighter blue colour (Fig. 2a). Separation of the boundary layer occurs at the angle of approximately 90° measured from the stagnant point 0° and indicated by widening of the darker blue zone. The obtained result is in accordance with the literature value for the experimental regime ($Re_c = 1000-200,000$) [22]. The formation of the wake and the reverse flow are visualized above the cylinder.

In the fluidized bed at the almost the same Re_c number (Fig. 2b), the concentration field is considerably more uniform and only a weak radial pattern around the cylinder can be observed. It can be concluded that movements of the particles in the fluidized bed significantly disturb formation and separation of the boundary layer. However, certain variations in the colour intensity indicates local distribution of mass transfer rates around the cylinder, which will be further analyzed by means of the values of local MTCs (Section 3.2).

Figures 3 and 4 show chromatograms during fluid flow around the cylinder in the presence of particles with a diameter of 1.2 mm and 2.1 mm, respectively.

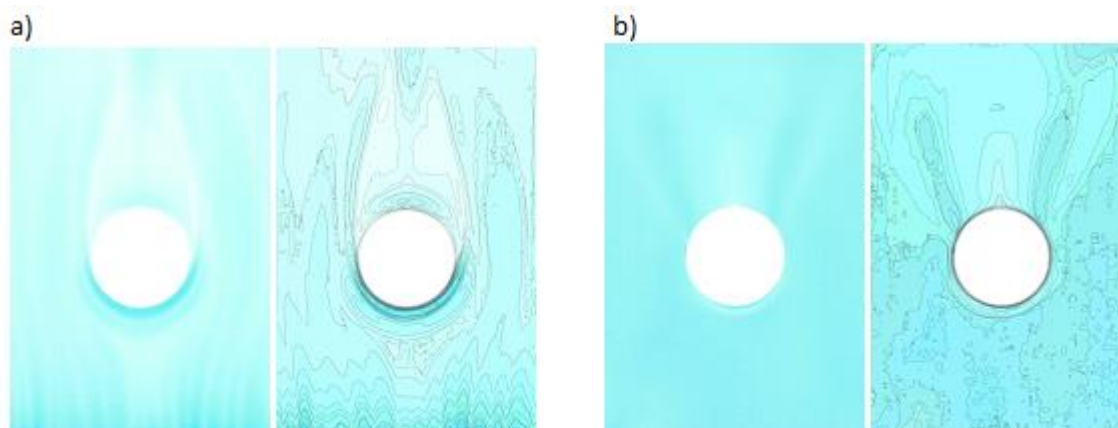


Figure 2. Scanned foils and chromatograms of concentration fields for: a) single phase flow ($U = 0.053 \text{ m s}^{-1}$, $Re_c = 1699$), b) fluidized bed, $d_p = 1.2 \text{ mm}$ ($U = 0.05 \text{ m s}^{-1}$, $Re_c = 1612$)

Figure 3a shows the flow around a cylinder in a packed bed of particles at the superficial velocity of $0.65 \cdot U_{mf}$. It is noted that the presence of the cylinder affects acceleration of the flow around it and that the individual particles which started to move even at that velocity, cannot be visually observed. Outside the zone close to the cylinder, stagnant particles are clearly visible with local staining around each individual particle. Figures 3b, 3c, and 3d show chromatograms in fluidized beds. At velocities slightly higher than the minimum fluidization velocity (Figure 3b, $U/U_{mf} = 1.2$), different staining can be observed around the cylinder, lighter at the bottom and the top of the cylinder and slightly darker on the sides. The lighter areas indicate lower mass transfer rates and lower flow velocities, which is especially pronounced at the top of the cylinder where the particles were in the packed state. With the increase in the superficial velocity (Fig. 3c, $U/U_{mf} = 2.9$; Fig. 3d, $U/U_{mf} = 4.2$) colour differences on the cylinder surfaces are less pronounced.

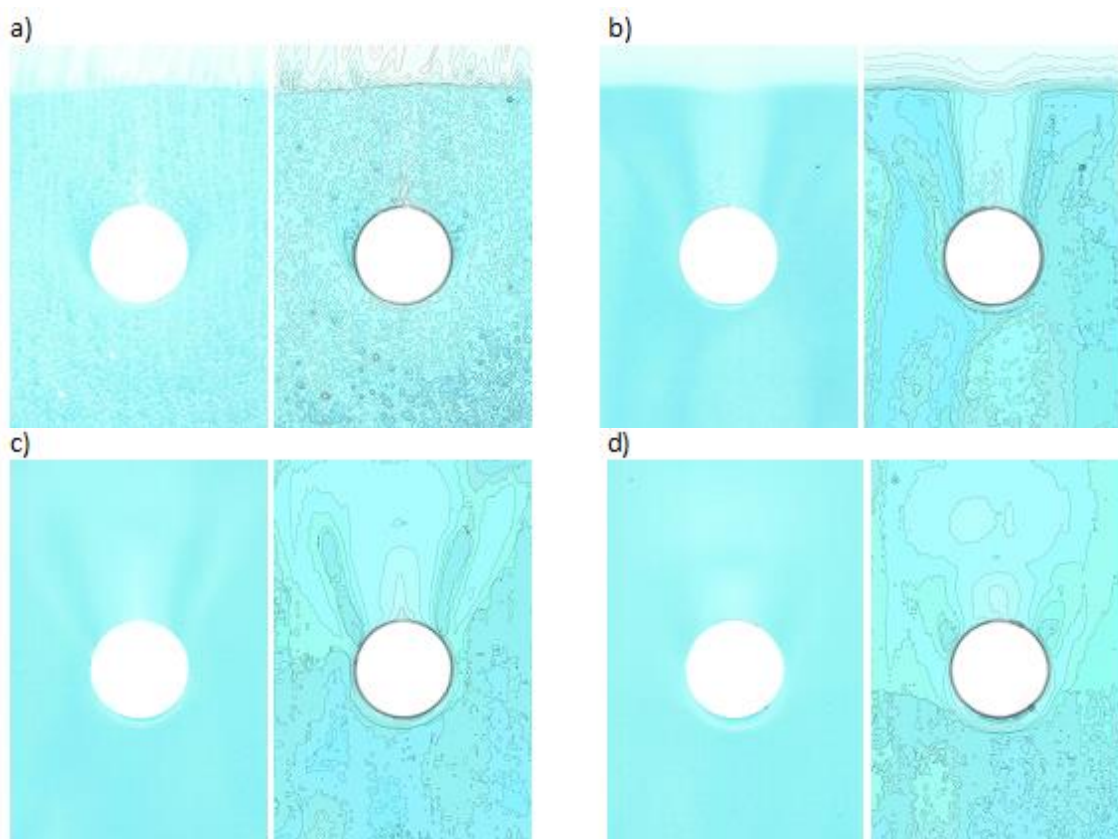


Figure 3. Scanned foils and chromatograms of concentration fields, $d_p = 1.2 \text{ mm}$: a) packed bed ($U = 0.011 \text{ m s}^{-1}$, $U/U_{mf} = 0.65$) and fluidized beds: b) $U = 0.021 \text{ m s}^{-1}$, $U/U_{mf} = 1.20$, c) $U = 0.05 \text{ m s}^{-1}$, $U/U_{mf} = 2.9$, d) $U = 0.071 \text{ m s}^{-1}$, $U/U_{mf} = 4.2$

Figure 4 shows chromatograms obtained in the presence of particles of 2.1 mm in diameter at fluid velocities in the range $U/U_{mf} = 0.67$ -4.1 regarding the minimum fluidization velocity. At a velocity lower than the minimum fluidization velocity (Fig. 4a), the influence of the cylinder on the movement of the particles has not been observed. All particles are in the packed bed, and the intensity of mass transfer and local flow around each particle can be clearly seen. At velocities higher than the minimum fluidization velocity ($U/U_{mf} = 1.4$, Fig. 4b), packed particles remain on the top of the cylinder. An approximately uniform staining of the surface can be observed at a velocity that is 2.6-fold of the minimum fluidization velocity (Fig. 4c). By further increasing the flow velocity ($U/U_{mf} = 4.1$, Fig. 4d) variations in the colour intensity appear again.

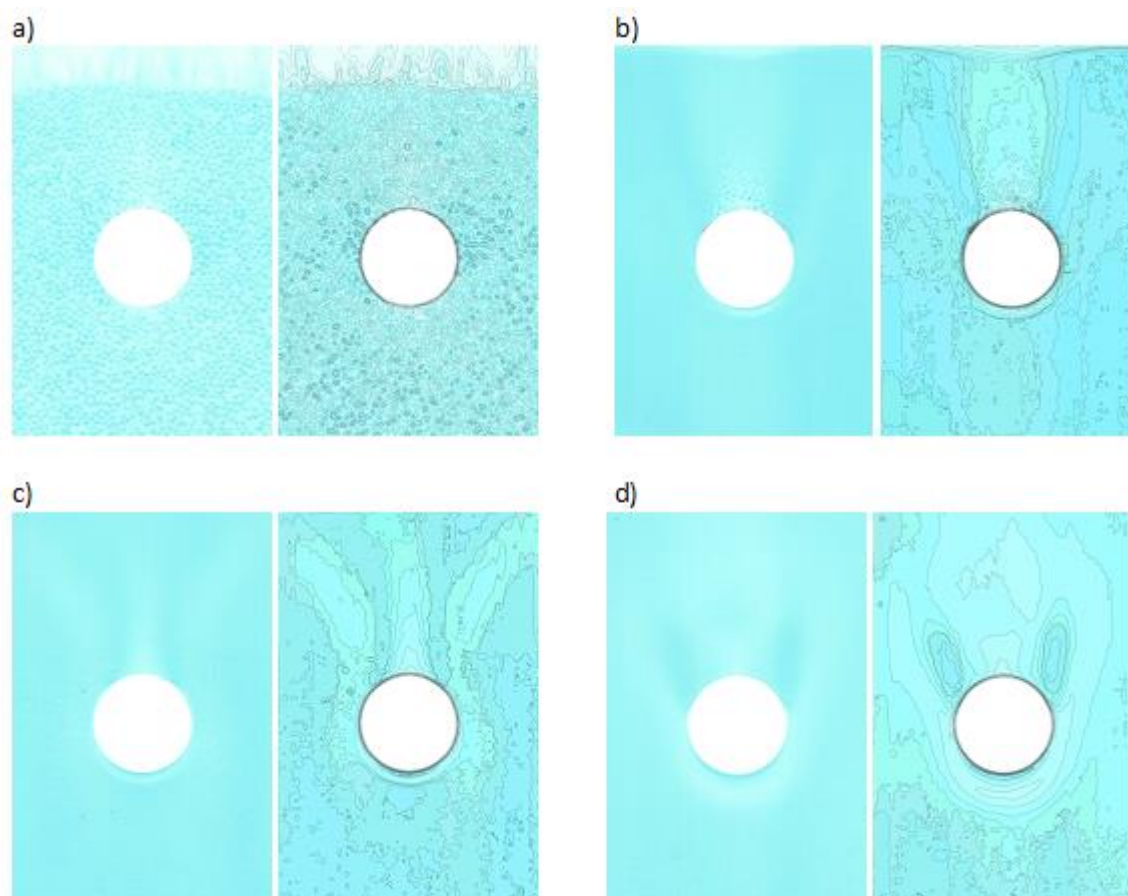


Figure 4. Scanned foils and chromatograms of concentration fields, $d_p=2.1$ mm: a) packed bed ($U = 0.018$ m s⁻¹, $U/U_{mf} = 0.67$) and fluidized beds: b) $U = 0.039$ m s⁻¹, $U/U_{mf} = 1.4$, c) $U = 0.064$ m s⁻¹, $U/U_{mf} = 2.6$, d) $U = 0.112$ m s⁻¹, $U/U_{mf} = 4.1$

3. 2. Local mass transfer coefficients

Local values of the mass transfer coefficient were obtained by analyzing foils at the surface of the cylinder. The appearance of the foils after the performed experiments is shown in Figure 5. The foil obtained in the single-phase flow is shown in Figure 5a while the foils obtained in the fluidized beds of particles of two investigated sizes are shown in Figures 5b and 5c at fluid velocities of about 0.05 m s⁻¹.

Based on the foils shown in Figure 5, by determining local color intensity values at each point with a step of 1°, local mass transfer coefficient values were determined, shown in Figure 6. In specific, Figure 6 represents the local MTCs around the cylinder as a function of the angular position (stagnant point is angle 0°) for the single-phase flow and for fluidized beds at almost the same superficial liquid velocity 0.05 m s⁻¹.

In the single phase flow the highest values of MTCs close to $6 \cdot 10^{-5}$ m s⁻¹ are observed at the bottom of the cylinder in the region between 0 and 40°. The zone between 40° and 90° is characterized by a sharp decrease of the MTCs down to the minimum of $0.2 \cdot 10^{-5}$ m s⁻¹ which has been attributed to the separation of the boundary layer [21]. In the zone between 90° and 180° a weak increase of MTCs has been observed.

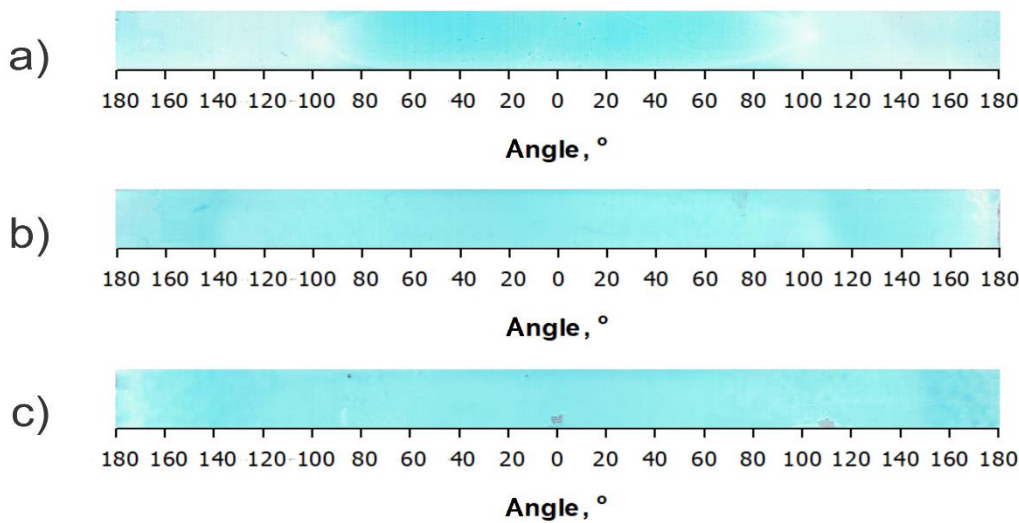


Figure 5. The appearance of foils at the surface of the cylinder in the single-phase flow (a) and in fluidized layers with particles with a diameter of 1.2 mm (b) and 2.1 mm (c). Angles are measured from the stagnant point 0°

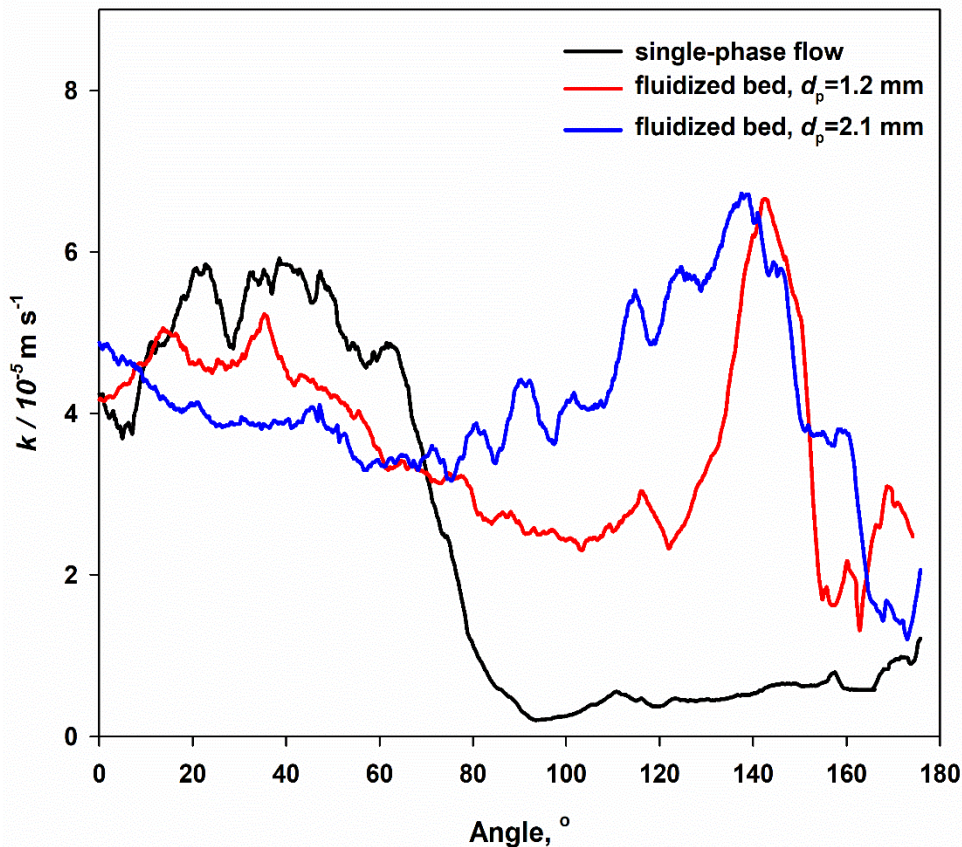


Figure 6. Local mass-transfer coefficient (k) around the cylinder for the superficial velocity of 0.05 m s^{-1} for the single phase flow and fluidized beds of two particle sizes

In the fluidized bed the local distribution of MTCs around the cylinder differs significantly from that in the single-phase flow. For the angular positions from 0 to 40° the values of MTCs are 20 to 30 % lower than in the single-phase flow. The minimum is not as pronounced as in the single-phase flow and occurs at the angle of 70° for 2.1 mm diameter particles and 100° for the 1.2 mm diameter particles. In the range 120 to 150° the values of MTCs in the fluidized bed are significantly higher than those in the single-phase flow and exhibit a sharp maximum at 140° . This maximum may be explained by intensified mixing of the particles in the region of angles 120 - 150° , which is caused by the increase in the particle

concentration and interstitial velocity (due to the presence of the cylinder) from one side and the reverse flow from another side. On the top of the cylinder (at angles 170 to 180°) the values of MTCs are low, but still slightly higher than those in the single-phase flow. The profiles of local MTCs for fluidized particles of the two investigated sizes (*i.e.* 1.2 and 2.1 mm in diameter) are quite similar, exhibiting a maximum at 140° in both cases.

Figure 7 represents the influence of the superficial liquid velocity on the local MTCs around the cylinder in the fluidized bed of 2.1 mm diameter particles. It can be observed that for the higher superficial velocities the values of MTCs are lower for all angular positions. It can be also clearly seen that for the higher velocities the minimum MTC is becoming more pronounced. That can be explained by the fact that for higher velocities particle concentration is lower and the separation of the boundary layer is less disturbed by particles. On the top of the cylinder the values of local MTCs are low for all tested superficial velocities.

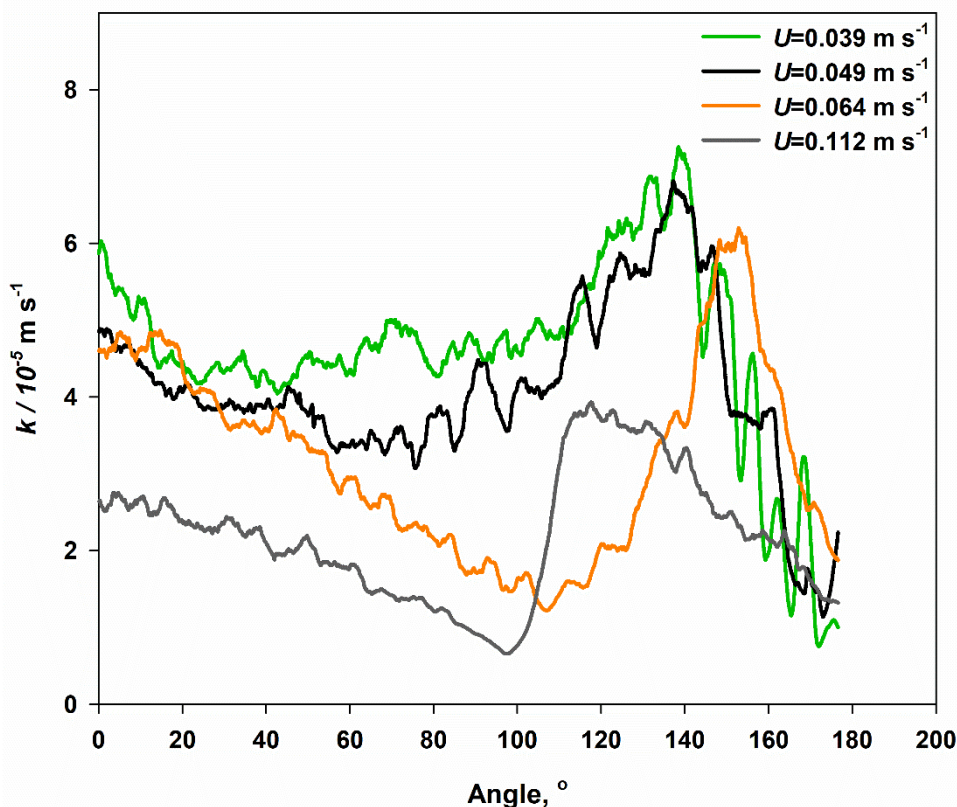


Figure 7. Influence of the superficial liquid velocity on local mass transfer coefficients around the cylinder ($d_p = 2.1 \text{ mm}$)

Local values of the Sherwood number for particle (Sh_p) were determined based on local MTC values, Figure 8 shows the local Sh_p values depending on the angular position for mass transfer in fluidized beds of particles with a diameter of 2.1 mm and at superficial velocities of 0.064 and 0.112 m s^{-1} . It could be observed that the local values of the Sh_p number decrease slightly up to the angle of about 90°, *i.e.* on the front half of the cylinder and increase sharply on the back half of the cylinder. Around the last point at the angle of about 180°, the Sh_p number values decrease.

3. 3. Average mass transfer coefficient

Based on the colouring intensity in foils at the cylinder surface, the average values of the mass transfer coefficients in single-phase flow and fluidized beds were calculated (Fig. 9). The results indicate that mass transfer coefficients increase with the increase in the superficial velocity for the single-phase flow. In fluidized beds, the trend is different, *i.e.* with the increase in the superficial velocity, the values of mass transfer coefficients slightly decrease. The largest difference in the coefficient values between the single-phase flow and the fluidized beds is at velocities close to the minimum fluidization velocity because at that point the particle concentration is the highest affecting mass transfer

better. However, differences in mass transfer intensities in the fluidized beds with particles of different sizes were not observed. It can be also seen in Figure 9 that at higher velocities when the porosity of the fluidized beds is high, the mass transfer coefficients are similar to that in the single-phase flow.

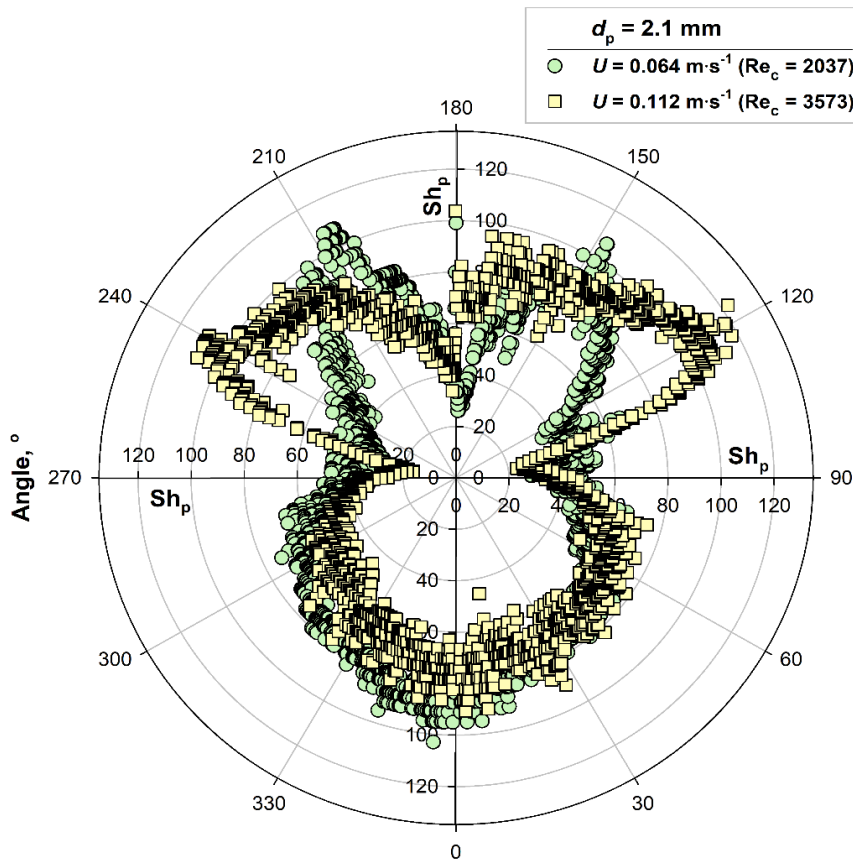


Figure 8. Local Sh_p number as a function of angular position in the fluidized bed of 2.1 mm particles at two fluid velocities

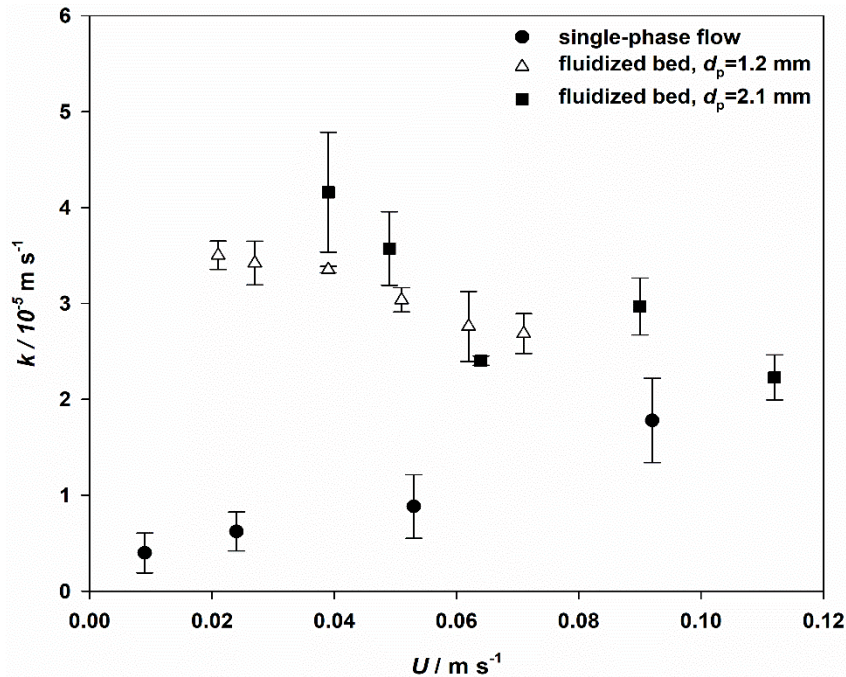


Figure 9. Average values of mass transfer coefficients as functions of the superficial fluid velocity in the single-phase flow and in fluidized beds of particles of two different sizes

3. 4. Comparison of experimental data with calculated values by literature correlations

Selected correlations (Table 3) were applied to calculate the dimensionless mass transfer factor in the range of experimental operating conditions (Table 2) and compare with the experimental data for average MTCs. The selected correlations are empirically derived from data obtained by different experimental techniques. Table 3 also shows average deviations between the experimental and calculated data. It could be seen that for the majority of correlations the calculated values are higher compared to the experimental values. Also, it could be noted that there are significantly smaller deviations for correlations obtained for the immersed object-fluid mass transfers, which is expected due to similar flow conditions. Two correlations of Storck and Vergnes [7] and Riba et al. [8] provided very good agreements with the experimental results.

Table 3. Selected literature correlations for calculation of the dimensionless mass transfer factor for immersed object-fluid and wall-fluid in the range of experimental operating conditions

Equation	Deviation / %	Ref.
Immersed object-fluid		
$j_D = 0.59 \left(\frac{Re_p}{1-\epsilon} \right)^{-0.44}$	5.0	[7]
$j_D = 0.264 Re_p^{-1.11} Ga^{0.36}$	-3.5	[8]
$j_D = 0.261 Ga^{0.324} Re_p^{-0.97}$	-30.3	[9]
$j_D = 0.64 \left(\frac{Re_p}{1-\epsilon} \right)^{-0.4}$	-28.3	[10]
Wall-fluid		
$j_D = 0.6 \left(\frac{Re_p}{1-\epsilon} \right)^{-0.5}$	30.4	[11]
$j_D = 0.4 Re_p^{-0.4}$	-26.8	[12]
$j_D = 0.14 Re_p^{-2/3} + 0.13 Re_p^{-4/3} Ar^{2/3} \frac{1-\epsilon}{1-\epsilon_0}$	-54.5	[13]

Comparisons of experimental and calculated values of the dimensionless mass transfer factor for the fluidized bed with 1.2 mm diameter particles are shown in Figure 10. As can be seen, the trend of dependence of j_D on the Re_p number is the same for experimental and calculated values and deviations between experimental and calculated values are larger for smaller Re_p numbers.

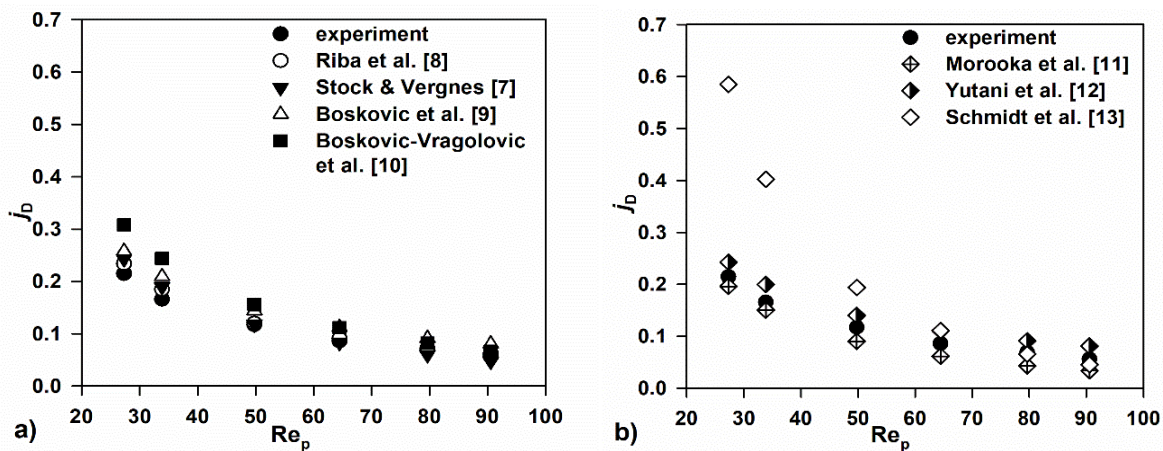


Figure 10. Comparison of experimental and calculated values of the mass transfer factor for the fluidized bed with 1.2 mm diameter particles

4. CONCLUSION

In this paper, mass transfer was experimentally investigated for the flow around a horizontal cylinder in the single-phase flow and in fluidized beds of particles of two sizes. Local and average values of mass transfer coefficients (MTCs) between the fluid and the immersed cylinder were determined by application of the adsorption method.

The local MTCs in the fluidized bed are higher than those in the single-phase flow for the angular positions 70 to 180°. Intensification of the mass transfer in the fluidized bed is especially pronounced at cylinder surfaces at the angular positions between 120 and 150°, with a sharp maximum at around 140°. Fluidized particles significantly disturb the structure of the boundary layer around the cylinder. Local MTCs in the fluidized bed have similar angular profiles for particles 1.2 and 2.1 mm in diameter. At higher superficial velocities the local MTCs in the fluidized bed are lower for all angular positions.

Values of the average mass transfer coefficients in fluidized beds did not depend on the particle diameter and decreased with the increase in the superficial velocity. The mass transfer coefficient in the fluidized bed is approximately 4-fold higher than that in the single-phase flow at the minimum fluidization velocity, while this difference decreases with the increase in fluid velocity, i.e. porosity of the fluidized bed.

Comparison of experimental values of mass transfer factors with values calculated by literature correlations of Storck and Vergnes [7] and Riba *et al.* [8] showed very good agreements with a mean deviation of 5 and -3.5 %, respectively.

The performed study showed the applicability of the adsorption method, novel results of local mass transfer coefficients on the immersed object and the suitability of certain tested correlations. It has also demonstrated the importance of optimizing the superficial fluid velocity as it has positive effects on particle mixing but negative effects on the mass transfer coefficient. The results and approach presented in this paper could be extended to other fluidized bed systems with immersed objects.

5. NOMENCLATURE

Ar	Archimedes number, $(g d_p \rho_f (\rho_f - \rho_p) / \mu^2)$
$c_0 / \text{kg m}^{-3}$	bulk concentration of methylene blue
$c_p / \text{kg m}^{-2}$	surface concentration of methylene blue on adsorbent layer
d_p / m	particle diameter
D / m	single cylinder diameter
$D_{AB} / \text{m}^2 \text{s}^{-1}$	the diffusion coefficient of the reactant
Ga	Galileo number, $(g d_p^3 \rho_f^3 / \mu^2)$
$G / \text{m s}^{-2}$	gravitational acceleration
j_D	dimensionless mass transfer factor, $(k Sc^{2/3} / U)$
$k / \text{m s}^{-1}$	mass transfer coefficient
Re_p	Reynolds number for particle, $(U d_p \rho_f / \mu)$
Re_c	Reynolds number for single cylinder, $(U D_p \rho_f / \mu)$
Sc	Schmidt number, $(m / \rho_f D_{AB})$
Sh_p	Sherwood number for particle, $(k d_p / D_{AB})$
t / s	exposure time
$U / \text{m s}^{-1}$	superficial fluid velocity
$U_{mf} / \text{m s}^{-1}$	minimum fluidization velocity
$U_t / \text{m s}^{-1}$	particle terminal velocity in a stagnant fluid
$\dot{V} / \text{dm}^3 \text{min}^{-1}$	fluid flowrate
<i>Greek letters</i>	
ϵ	bed porosity
ϵ_0	packed bed porosity
ϵ_{mf}	bed porosity at minimum fluidization velocity
$\mu / \text{mPa s}$	fluid viscosity
$\rho_f / \text{kg m}^{-3}$	fluid density
$\rho_p / \text{kg m}^{-3}$	particle density

Acknowledgements: This work was financially supported by the Ministry of Science, Technological Development and Innovation of the Republic of Serbia (Grant No. 451-03-65/2024-03/200135 and Grant No. 451-03-66/2024-03/200026).

REFERENCES

- [1] Rasoulnia P, Hajdu-Rahkama R, Puhakka JA. High-rate and -yield continuous fluidized-bed bioconversion of glucose-to-gluconic acid for enhanced metal leaching. *Chem Eng J.* 2023; 462: 142088 <https://doi.org/10.1016/j.cej.2023.142088>
- [2] Gui L, Yang H, Huang H, Hu, C, Feng Y, Wang X. Liquid solid fluidized bed crystallization granulation technology: Development, applications, properties, and prospects. *J Water Process Eng.* 2022; 45: 102513 <https://doi.org/10.1016/j.jwpe.2021.102513>
- [3] Kalaga DV, Dhar A, Dalvi SV, Joshi JB. Particle-liquid mass transfer in solid-liquid fluidized beds. *Chem Eng J.* 2014; 245: 323-341 <https://doi.org/10.1016/j.cej.2014.02.038>
- [4] Evans GC, Gerald CF. Mass transfer from benzoic acid granules to water in fixed and fluidized beds at low Reynolds numbers. *Chem Eng Progr.* 1953; 49: 135-140; ISSN: 0360-7275
- [5] Upadhyay SN, Tripathi G. Liquid phase mass transfer in fixed and fluidized beds of large particles. *J Chem Eng Data.* 1975; 1: 20-26 <https://doi.org/10.1021/je60064a001>
- [6] Shen GC, Geankoplis CJ, Brodkey RS. A note on particle-liquid mass transfer in a fluidized bed of small irregular-shaped benzoic acid particles *Chem Eng Sci.* 1985; 40: 1797-1802 [https://doi.org/10.1016/0009-2509\(85\)80046-4](https://doi.org/10.1016/0009-2509(85)80046-4)
- [7] Storck A, Vergnes F. Transfert de Matiere entre un Electrolyte et une Paroi Cylindrique Immergee dans un Lit Fluidise Liquide-Solide: Influence de la Masse Volumique des Particules Fluidisees. *Powder Techn.* 1975; 12209-2013 [https://doi.org/10.1016/0032-5910\(75\)85019-4](https://doi.org/10.1016/0032-5910(75)85019-4)
- [8] Riba, JP, Routie R, and Couderc JP. Mass transfer from a fixed sphere to liquid in a fluidized bed. In: *Fluidization: Proceedings of the Second Engineering Foundation Conference.* Trinity College, Cambridge, England, 1978. pp 157-162
- [9] Bošković N, Grbavčić BŽ, Vuković VD, Marković-Grbavčić M. Mass Transfer between Fluid and Immersed Surfaces in Liquid Fluidized beds of Coarse Spherical Inert Particles. *Powder Techn.* 1994; 79: 217-225 [https://doi.org/10.1016/0032-5910\(94\)02826-5](https://doi.org/10.1016/0032-5910(94)02826-5)
- [10] Bošković-Vragolović N, Brzić D, Grbavčić Ž. Mass Transfer between Fluid and Immersed Object in liquid-solid packed and fluidized beds. *J Chem Soc.* 2005; 70: 1273-1379 <https://doi.org/10.2298/JSC0511373B>
- [11] Morooka S, Kusakabe K, Kato Y, Mass Transfer Coefficient at Wall of Rectangular Fluidized Beds for Liquid—Solid and Gas—Liquid—Solid Systems. *Kagaku Kogaku Ronbunshu.* 1979; 5 (2): 162-166 <https://doi.org/10.1252/kakoronbunshu.5.162>
- [12] Yutani N, Ototake N, Fan LT. Statistical Analysis of Mass Transfe in Liquid-Solid Fluidized Beds. *Ind Eng Chem Res.* 1987;26: 343-347 <https://doi.org/10.1021/ie00062a028>
- [13] Schmidt S, Buchs J, Born C, Biselli M, A New Correlation for the Wall-to-Fluid Mass Transfer in Liquid-Solid Fluidized Beds. *Chem Eng Sci.* 1999; 54: 829-839 [https://doi.org/10.1016/S0009-2509\(98\)00284-X](https://doi.org/10.1016/S0009-2509(98)00284-X)
- [14] Kim J, Kim K, Ye H, Lee E, Shin C, McCarty PL, Bae J. Anaerobic Fluidized Bed Membrane Bioreactor for Wastewater Treatment. *Env Sci Tech.* 2011; 45 (2): 576-581 <https://doi.org/10.1021/es1027103>
- [15] Perry SC, De Leon CP, Walsh FC. Review—The Design, Performance and Continuing Development of Electrochemical Reactors for Clean Electrosynthesis. *J Electrochem Soc.* 2020; 167: 155525; <https://doi.org/10.1149/1945-7111/abc58e>
- [16] Garim MM, Freire JT, Goldstein RJ. Local mass transfer coefficients around a cylinder in a fluidized bed. *Powder Technol.* 1999; 101 (2): 134-141 [https://doi.org/10.1016/S0032-5910\(98\)00164-8](https://doi.org/10.1016/S0032-5910(98)00164-8)
- [17] Di Natale F, Nigro R. A critical comparison between local heat and mass transfer coefficients of horizontal cylinders immersed in bubbling fluidized beds. *Int. J Heat Mass Tran.* 2012; 55 (25-26): 8178-8183 <https://doi.org/10.1016/j.ijheatmasstransfer.2012.08.002>
- [18] Končar-Đurđević S. Application of a new adsorption method in the study of flow of fluids. *Nature.*1953; 172: 858 <https://doi.org/10.1038/172858a0>
- [19] Mitrović M. Transport phenomena in multiphase systems. *J Serb Chem Soc.* 1996; 61: 233- 251, ISSN: 0352-5139
- [20] Bošković-Vragolović N, Garić-Grulović R, Grbavčić Ž, Pjanović R. Mass transfer in heterogeneous systems by adsorption method. *CI CEQ,* 2009; 15 (1): 25-28 <https://doi.org/10.2298/CICEQ0901025B>

- [21] Bošković-Vragolović N, Garić-Grulović R, Pjanović R, Grbavčić Ž. Mass transfer and fluid flow visualization for single cylinder by the adsorption method. *Int. J. Heat Mass Trans.* 2013; 59: 155-160
<https://doi.org/10.1016/j.ijheatmasstransfer.2012.11.077>
- [22] Welty RJ, Wicks EC, Wilson ER, Rorrer G. *Fundamentals of Momentum, Heat, and Mass Transfer*. 5th ed., Copyright 2008 John Wiley & Sons, Inc. ISBN: 13 978-0470128688

Lokalni prenos mase i vizualizacija toka oko cilindra u fluidizovanom sloju tečno-čvrsto

Nevenka M. Bošković-Vragolović¹, Danica V. Brzić¹, Katarina S. Šućurović², Rada V. Pjanović¹,
Darko R. Jaćimovski² i Radmila V. Garić-Grulović²

¹Univerzitet u Beogradu, Tehnološko-metalurški fakultet, Beograd, Srbija

²Univerzitet u Beogradu, Institut za hemiju, tehnologiju i metalurgiju – Institut od nacionalnog značaja za Republiku Srbiju, Beograd, Srbija

(Naučni rad)

Izvod

U ovom radu je primenjena adsorpciona metoda za vizualizaciju strujanja i određivanje lokalnih i srednjih koeficijenata prenosa mase na horizontalni cilindar u tečno-čvrsto fluidizovanom sloju. Dobijena polja koncentracije na adsorbentu (folije silika gela) predstavljaju kvalitativnu sliku strujanja oko cilindra. Poređenjem koncentracionih polja oko cilindra u jednofaznom toku i u fluidizovanom sloju, uočeno je da fluidizovane čestice značajno ometaju formiranje i odvajanje graničnog sloja. Lokalni koeficijenti prenosa mase su značajno zavisili od ugaonog položaja tačke na površini cilindra i pokazali su maksimum pri uglu 140° (mereno u odnosu na zaustavnu tačku koja predstavlja ugao od 0°). Odabrane korelacije su primenjene za predviđanje prosečnih vrednosti koeficijenata prenosa mase, a dve najbolje su pokazivale odstupanja od eksperimentalnih podataka do 5 %.

Ključne reči: koeficijent prenosa mase; adsorpciona metoda; opstrujavanje cilindra; koncentraciona polja

